Preparation of Antibacterial Dialdehyde Nanocellulose Using LiBr·3H$_2$O Non-Dissolving Pretreatment Promoted Periodate Oxidation

Zhang, Yidong; Deng, Wangfang; Liu, Chao; Yan, Fei; Wu, Meiyan; Cui, Qiu; Willför, Stefan; Xu, Chunlin; Li, Bin

Published in:
ACS Sustainable Chemistry and Engineering

DOI:
10.1021/acssuschemeng.2c07746
10.1021/acssuschemeng.2c07746
10.1021/acssuschemeng.2c07746

Published: 01/05/2023

Document Version
Final published version

Document License
CC BY

ACS Sustainable Chemistry & Engineering

pubs.acs.org/journal/ascecg

Research Article

Preparation of Antibacterial Dialdehyde Nanocellulose Using $LiBr{\cdot}3H_2O$ Non-Dissolving Pretreatment Promoted Periodate Oxidation

Yidong Zhang,[#] Wangfang Deng,[#] Chao Liu, Fei Yan, Meiyan Wu, Qiu Cui, Stefan Willför, Chunlin Xu,* and Bin Li*

Cite This: *ACS Sustainable Chem. Eng.* 2023, 11, 6641−6651

Read Online

ACCESS | Metrics & More | Article Recommendations | Supporting Information

ABSTRACT: Dialdehyde nanocellulose (DANC), obtained via periodate oxidation, has been widely used in foods, cosmetics, and biomedical fields due to its unique characteristics. However, the high-crystallinity and tight structure of cellulose retards the efficiency of periodate oxidation for producing DANC. Herein, a novel sustainable and clean approach with less energy consumption and low cost was developed through $LiBr{\cdot}3H_2O$ (LBTH) non-dissolving pretreatment, which can shorten the oxidation time of the followed periodate oxidation and reduce the oxidant consumption. It was shown that the cellulose Iβ structure of hardwood dissolving pulp (HDP) was largely transformed into an amorphous structure after LBTH non-dissolving pretreatment for 30 min, and the corresponding crystallinity of HDP was reduced from 83.2 to 48.7%. After pretreatment for 60 min, the aldehyde group content of the obtained DANC increased by around 30% compared to the control without pretreatment while the operational cost was reduced by 45%. Moreover, the fabricated DANC showed strong antibacterial activity against both *Escherichia coli* and *Bacillus subtilis*. LBTH was recovered and reused, and the pretreatment effectiveness was also maintained. This study provides a sustainable, cost-effective, and clean approach for the preparation of DANC and will promote the application of cellulose nanomaterials.

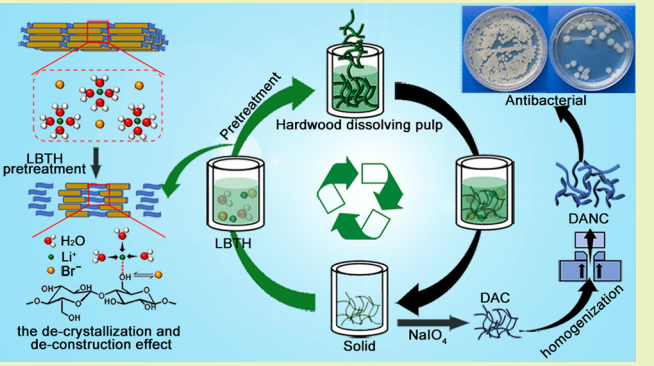

KEYWORDS: *molten salt hydrate, dialdehyde nanocellulose, cellulose accessibility, antibacterial, cleaner technology, sustainable process*

INTRODUCTION

Cellulose derived from various plants such as trees, bamboo, hemp, cotton, agricultural crops, and marine algae can be converted into various chemicals or functional materials by hydrolysis or derivatization.[1−6] Among the cellulose derivatives, dialdehyde nanocellulose (DANC) with unique structure and properties is an interesting nanomaterial thanks to its wide application potential.[7−13] DANC can be obtained through the oxidation between cellulose and sodium periodate ($NaIO_4$) followed by high-pressure homogenization.[14,15] In this reaction, the vicinal 2,3-hydroxyl groups of cellulose units can be oxidized to aldehyde groups, which can further react with carbonyl/hydroxyl groups or amino groups by aldol reactions or Schiff base crosslinking to fabricate diverse functional materials, such as absorbents,[7−9] stabilizer of protein,[10] drug carriers,[11] tissue engineering scaffolds,[12] and immobilized antibodies.[13] It was reported that DANC/silver nanoparticle composites prepared through the microwave-assisted hydrothermal method can be used in biomedical fields.[16] Moreover, DANC/chitosan films were fabricated by the solution casting technique and can be applied in the areas of food packaging and biomedical treatments.[15] Also, hydrogels with antibacterial activity were developed from DANC, xylan, and silver nitrate via a three-step process, which can be used as the wound dressing materials toward medical treatment.[17−19] Moreover, dialdehyde amylopectin/chitosan nanoparticles fabricated by the Schiff base reaction was employed to stabilize high internal phase Pickering emulsions with various oils.[20] However, the reaction efficiency of oxidation was quite low and the required dosage of $NaIO_4$ was high (1−5 mol per mol of anhydroglucose unit (AGU)),[15,21] due to the highly dense and crystalline structure of cellulose created by the strong intermolecular and intramolecular bonds.[22] In addition, $NaIO_4$ is expensive so its usage should be reduced, which can also lead to less

Received: December 31, 2022
Revised: March 31, 2023
Published: April 16, 2023

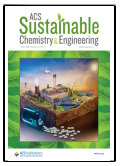

https://doi.org/10.1021/acssuschemeng.2c07746
ACS Sustainable Chem. Eng. 2023, 11, 6641−6651

environment impact.[23] Hence, there is a need to improve accessibility to cellulose to promote the reaction efficiency of periodate oxidation with reduced oxidant consumption, ensuring a sustainable and safe process.

To increase the reaction efficiency of cellulose, an activation pretreatment of cellulose is usually carried out, using chemicals such as concentrated alkali, ionic liquids (ILs), deep eutectic solvents (DESs), or molten salt hydrates (MSHs).[24,25] Compared to other cellulose solvents, MSHs have some unique properties such as easy recycling, low viscosity, nontoxicity, low vapor pressure, and high boiling point.[26,27] MSH is a concentrated aqueous solution of inorganic salts, in which the molar ratio of water to salt is close to the coordination number of salt cations.[28] MSH is also called inorganic IL ascribed to its similar properties to organic ILs. Compared with organic ILs, MSH complexes are non-toxic, green, and low sensitive to water.[29] In recent years, some MSHs have been used for activation of cellulose, such as $ZnCl_2$·3-4H_2O, LiBr·3H_2O, $LiClO_4$·3H_2O, and LiI_2·H_2O.[30] For example, cellulose nanofibers with excellent flame-retardant and catalytic properties were fabricated by $ZnCl_2$ pretreatment.[31] Moreover, LiBr·3H_2O (LBTH) has been identified as a green solvent for swelling, dissolution, or degradation of cellulose.[32] It was reported that some lithium ions can diffuse into the crystalline region of cellulose and promote the separation of cellulose chains.[27,32] The free bromine anion outside the hydrosphere is bonded to the hydrogen of a cellulose hydroxyl to prevent the reconstitution of hydrogen bonds between cellulose chains.[26,33] It was also reported that microcrystalline cellulose (MCC) after LBTH pretreatment (without dissolution of cellulose) at room temperature can be near completely saccharified into glucose (98.3%) with a very low enzyme dosage (2.5 mg protein/g-glucan) due to the deconstructed and loosen structure of MCC by LBTH, while the untreated MCC under the same saccharification conditions exhibited a low conversation (16.7%).[34] Thus, it is expected that LBTH non-dissolving pretreatment (without dissolution of cellulose) can increase the accessibility of dissolving pulp fibers with the same deconstruction effect as the LBTH pretreatment of MCC and can be beneficial to the fabrication of DANC.

Therefore, to verify this hypothesis, in this work the effectiveness of LBTH non-dissolving pretreatment of hardwood dissolving pulp (HDP) was comprehensively investigated, and the LBTH-pretreated HDP with increased accessibility was used to prepare DANC with less energy consumption and reduced oxidant dosage. Moreover, the recovery and reuse approaches of the LBTH solution were assessed as well, and the schematic flowchart of the LBTH non-dissolving pretreatment of cellulose at room temperature is exhibited in Figure 1. This fundamental study will provide a new strategy of high-efficiency pretreatment for the fabrication of cellulose derivatives (e.g., DANC) and cellulose nanomaterials.

EXPERIMENTAL SECTION

Materials. HDP (cellulose 98 ± 0.5%; hemicellulose 1 ± 0.2%; lignin less than 0.1%, respectively) was kindly provided by Mudanjiang Hengfeng Paper Co., Ltd. (China). Lithium bromide (LiBr, ≥99%) and $NaIO_4$ (≥99.5%) were purchased from Aladdin Reagents (China). Luria-Bertani (LB) Nutrient Agar was purchased from Beijing Solarbio Science & Technology Co., Ltd. (China). Methanol (≥99%), sodium hydroxide (≥95%), and thymol blue (≥99%) were bought from Sinopharm Group Chemical Reagent Co., Ltd. (China). They were used without further purification.

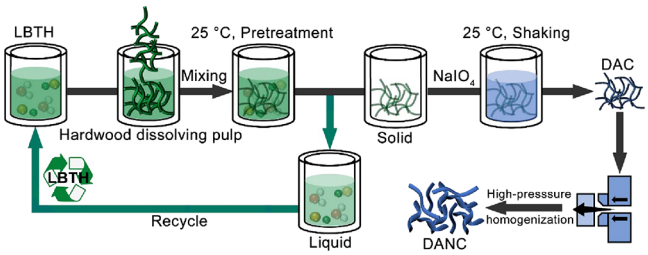

Figure 1. Schematic diagram of the preparation method of DANC with LBTH non-dissolving pretreatment.

MSH Pretreatment. Two grams of HDP and 20 g of LBTH were first added to a 250 mL glass bottle and left at room temperature (25 °C) to pretreat HDP for a certain time (0−60 min). After that, the HDP suspension was filtrated under vacuum for solid−liquid separation. The filtrate was LBTH and collected for reuse. The collected cellulosic solids were washed with deionized water until the conductivity of the filtrate was below 10 μS cm^{-1}. The solid content and yield of cellulose samples after washing were measured. The pretreated HDP cellulose samples were stored in a wet state in a refrigerator (4 °C) for subsequent characterization and modification.

Preparation of DANC. The preparation of DANC was proceeded according to a reported work with slight modification.[35] As shown in Figure 1, 1 g of LBTH-pretreated HDP cellulose, 100 g of water, and 1.6 g of $NaIO_4$ (1.2 mol per mol of AGU) were mixed and stirred in the dark for various reaction times (0−48 h), and the time-dependent data were gained by sampling a certain amount of reaction mixture at regular intervals. After sampling, the products were washed four times by centrifugation (1096 × g) with deionized water to obtain pure dialdehyde cellulose. The solid content and yield of cellulose samples after washing were measured by weight percentage. After that, the oxidized cellulose samples were re-dispersed in water with a consistency of 0.2 wt % and then passed through an ATS-BASIC homogenizer (AH-PILOT 2015, ATS Engineering Ltd., China) five times at 600 bars to obtain DANC.

The DANC sample was named as Lx, y, z, where, x, y, and z represent the pretreatment time of LBTH (min), the amounts of periodate (mol), and the reaction time (h), respectively.

Determination of Aldehyde Content. The aldehyde content of DANC was determined according to a previous report.[14] The freeze-dried samples were mixed with 5 wt % hydroxylamine hydrochloride methanol solution. Then, the mixture was shaken at 100 rpm at room temperature (25 °C) with thymol blue to react for 5 h. After that, the solution was titrated with NaOH methanol solution (0.03 M) until the indicator turned from red to yellow and no discoloration within 30 s. The aldehyde content is calculated by the following equation:

$$[\mathrm{CHO}] = \frac{(V_2 - V_1) \times C_{\mathrm{NaOH}}}{m_{\mathrm{DANC}}} \quad (1)$$

where, [CHO] is the aldehyde content of DANC (mmol/g), V_1 is the volume of NaOH methanol solution required for titration of the pulp suspension (mL), V_2 is the volume of NaOH methanol solution required for titration of the DANC suspension (mL), C_{NaOH} is the concentration of NaOH methanol solution (0.03 M), and m_{DANC} is the weight of DANC (g).

Characterization. The cellulose samples were characterized by Fourier transform infrared (FTIR) spectroscopy, X-ray diffraction (XRD), scanning electron microscopy (SEM), transmission electron microscopy (TEM), thermogravimetric analysis (TGA), zeta potential, degree of polymerization (DP), and antibacterial tests. The detailed information is found in the Supporting Information document.

RESULTS AND DISCUSSION

Microstructure and Crystal Structure of HDP. It is known that cellulose with a high crystalline and dense structure

https://doi.org/10.1021/acssuschemeng.2c07746
ACS Sustainable Chem. Eng. 2023, 11, 6641−6651

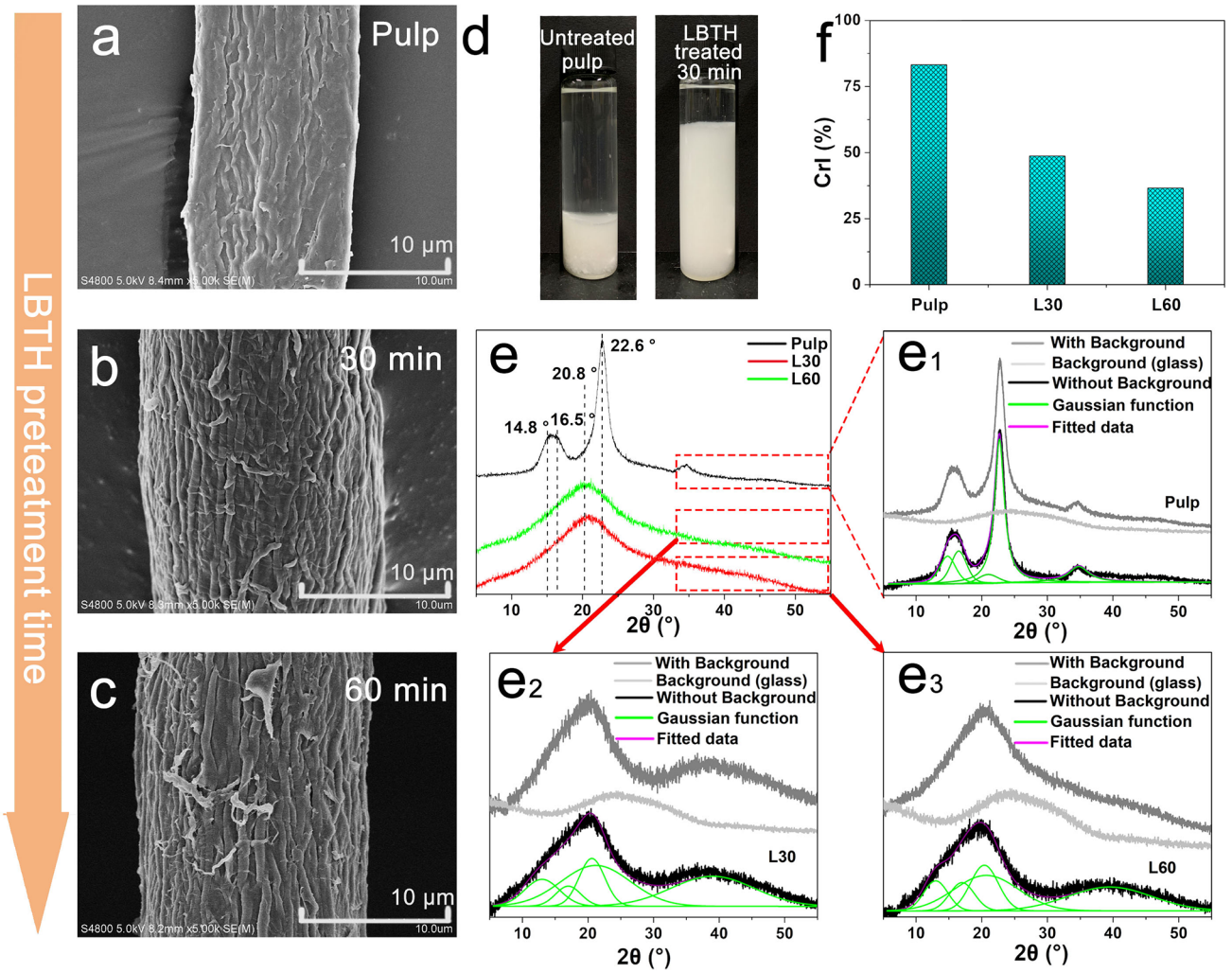

Figure 2. Microstructure and crystal structure of HDP. SEM images of the original HDP (a); HDP after LBTH pretreatment (b, 30 min; c, 60 min); photo (d) of untreated HDP in water (1%) and pretreated cellulose (with LBTH at 25 °C for 30 min) in water (1%); XRD patterns (e) and profile fitting (peak deconvolution method) of XRD patterns (e_1, e_2, and e_3) of HDP and the sample after LBTH pretreatment; *CrI* (f) of HDP and the sample after LBTH pretreatment (L30, HDP sample after LBTH pretreatment for 30 min; L60, HDP sample after LBTH pretreatment for 60 min).

can hinder the hydrolysis or functional modification of cellulose. In this work, HDP was pretreated with LBTH at room temperature for increasing the accessibility of cellulose. As shown in Figure S1, HDP was insoluble in LBTH for 60 min and the slight loss of cellulose (around 1.5%) after LBTH pretreatment was attributed to the washing process. The SEM images of HDP after LBTH pretreatment with different reaction times are shown in Figure 2 and Figure S2. Compared with the relatively compact and dense surface structure of the flat original HDP (Figure 2a), a wrinkled surface and swelled cellulose fibers were observed after the LBTH pretreatment (Figure 2b,c). With the increasing of LBTH pretreatment time, more and more deconstruction occurred on the surface of the fibers and the surface of HDP was remarkably changed. The morphology of the fibers showed that the LBTH pretreatment had strong surface deconstruction ability for HDP at room temperature. Similar phenomena were reported on the LBTH non-dissolving pretreatment of MCC.[34] Furthermore, as shown in Figure 2d, the sample after LBTH pretreatment for 30 min formed a thick and flocky layer in water due to the swelling of pulp fibers, while the untreated pulp was deposited forming a thin precipitate at the bottom in water.

XRD was used to further investigate the crystalline structure of cellulose after LBTH non-dissolving pretreatment. As shown in Figure 2e, the XRD patterns of cellulose samples without LBTH pretreatment showed typical peaks at 14.8, 16.5, and 22.6°, which were consistent with peaks of cellulose Iβ.[36,37] On the other hand, the XRD patterns of samples after LBTH pretreatment only presented a broad highly amorphous peak located at 20.8°, which is consistent with the previously reported maximum peak of typical amorphous cellulose regenerated by ILs.[34,38] According to the peak deconvolution method, the *CrI* values of HDP, the sample after LBTH pretreatment for 30 min (L30), and the samples after LBTH pretreatment for 60 min (L60) were 83.23, 48.70, and 36.56%, respectively (Figure 2f). Thus, after LBTH pretreatment, the crystalline structure of HDP was changed from cellulose Iβ to a highly amorphous structure, and the crystallinity of cellulose clearly decreased due to the de-crystallization and de-construction effect of LBTH on HDP.

ATR-FTIR, DP, and TG were used to further investigate the molecular structural changes and thermal stability of cellulose after pretreatment. The band of O−H stretching vibration shifted to a higher wavenumber (from 3412 to 3443 cm^{-1}),

https://doi.org/10.1021/acssuschemeng.2c07746
ACS Sustainable Chem. Eng. 2023, 11, 6641−6651

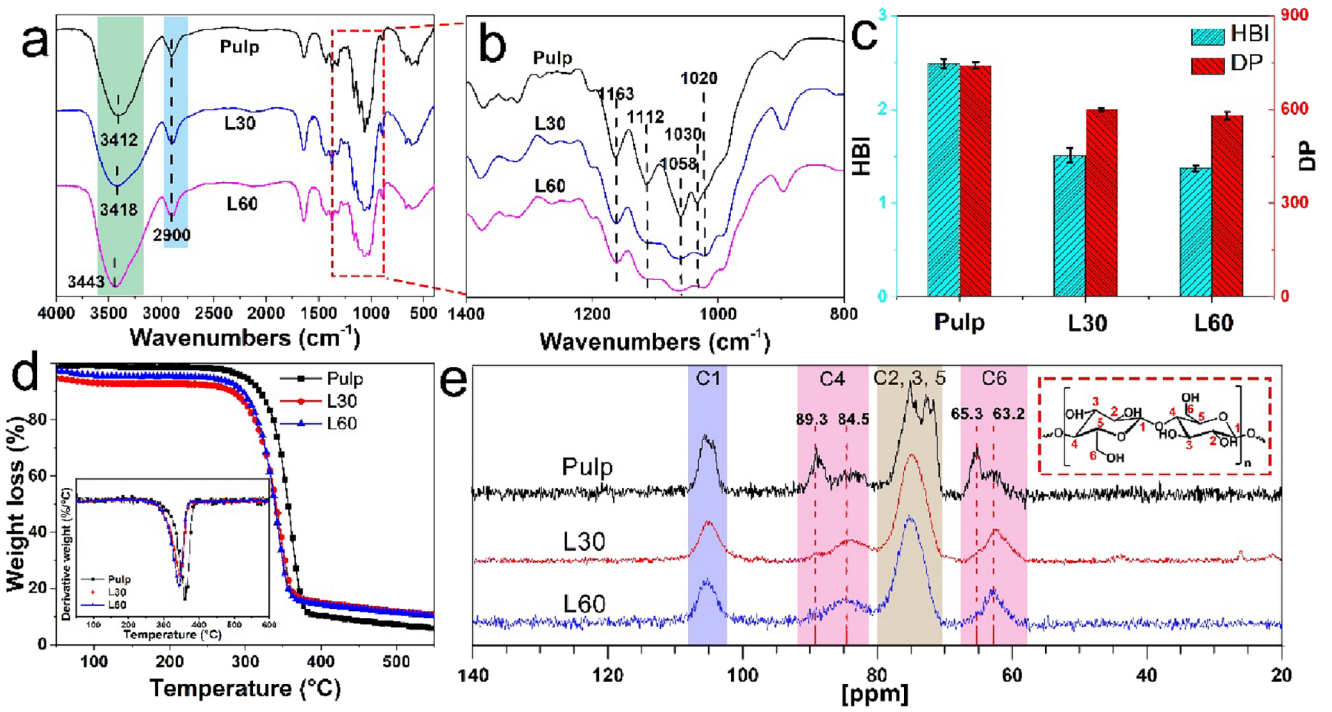

Figure 3. Property characterization of HDP and the samples after LBTH pretreatment. FTIR spectra (a), partial FTIR spectra (b), DP (c), hydrogen-bond intensity (c), TG (d), DTG (d), and 13C NMR-spectra (e) curves of HDP and the sample after LBTH pretreatment (L30, HDP sample after LBTH pretreatment for 30 min; L60, HDP sample after LBTH pretreatment for 60 min).

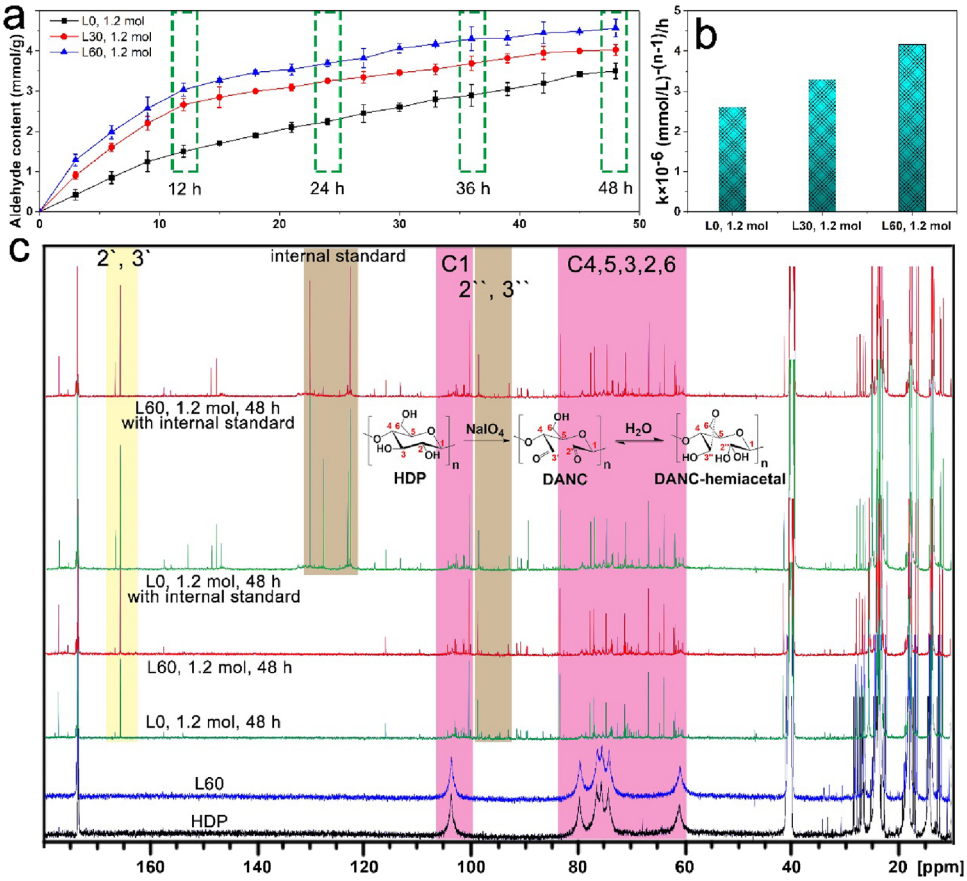

Figure 4. Kinetic study (a, b) of preparation of DANC; (c) quantitative 13C NMR spectra of HDP, L60, and DANC samples.

which was probably due to the reduced hydrogen bonding in cellulose after LBTH pretreatment (Figure 3a).[39] Moreover, the band of C−O−C pyranose ring skeletal vibrations shifted from 1030 to 1020 cm^{-1}, which suggested the change of the

https://doi.org/10.1021/acssuschemeng.2c07746
ACS Sustainable Chem. Eng. 2023, 11, 6641−6651

crystalline structure of cellulose after LBTH pretreatment (Figure 3b).[34] As shown in Figure S3, the obtained FTIR spectra of all samples were zoomed in (3800−3000 cm^{-1}) to evaluate the changes of hydrogen bonding based on the peak-differentiating and imitating method. The fit peaks in the spectra of 3400 cm^{-1} belong to the O−H stretching of hydroxyl groups in the cellulose chain, and the fit peaks around 3244 cm^{-1} belong to hydrogen bonds in the inter- and intramolecular bonds of cellulose.[40,41] As evident, the fit peaks of the O−H stretching and hydrogen bonds shift to the higher wavenumbers (3400−3500 cm^{-1}) appearing in the spectra of sample after LBTH pretreatment. As we know, decreased hydrogen bonding can cause the movement of peak position to a higher wavenumber and the peak broadening in FTIR spectra of samples.[40,41]

In addition, the changes in the DP of cellulose after LBTH pretreatment are shown in Figure 3c. It was found that the DP of cellulose decreased slightly from 750 to 600 after LBTH pretreatment at room temperature. The decrease in DP confirmed that the LBTH pretreatment can slightly break the glycosidic bonds of cellulose under room temperature and pressure, which can effectively improve cellulose accessibility and decrease crystallinity. Furthermore, the hydrogen-bond intensity of pulp and the samples after LBTH pretreatment were calculated using the FTIR A_{3308}/A_{1330}.[42] The hydrogen-bond intensity (HBI) of cellulose decreased 44% (from 2.5 to 1.4) after LBTH pretreatment, which was caused by the changes of hydrogen bonds (Figure 3c).

As shown in TG curves (Figure 3d), the initial decomposition temperature (onset temperature, T_o) of HDP was 338.8 °C and the maximum degradation rate (peak temperature, T_{max}) reached 360.1 °C. As evident, the T_o and T_{max} of samples after LBTH pretreatment were lower than those of HDP. The relatively lower T_o and T_{max} of samples were related to their relatively low crystallinity, loose structure, and DP in comparison with HDP. Furthermore, compared with HDP, the residue amounts of samples with LBTH non-dissolving pretreatment clearly increased (Table S1). This result was because the easier decomposition of the samples after LBTH pretreatment tended to generate thermally stable char easily.[43] Figure 3e shows the 13C spectra of HDP, L30, and L60. The peaks at 89.3 and 65.3 ppm were assigned to crystalline regions, while the peaks at 84.5 and 63.2 ppm were assigned to amorphous regions.[44−46] Compared to HDP, a significant change in the signal intensity can be seen in crystalline regions of the samples after LBTH pretreatment, which further confirmed the de-crystallization and de-construction effects of LBTH on HDP.

Periodate Oxidation. To further verify the effect of LBTH non-dissolving pretreatment, a kinetic study for the preparation of DANC and the characterizations of the obtained DANC were carried out, and the results are shown in Figure 4, Table 1, and Tables S2 and S3. Kinetic study as a mathematical tool is of great importance to optimize the production conditions of DANC toward large-scale processes.[47] The k values of samples after LBTH pretreatment were higher than those of unpretreated HDP (Figure 4b). The relatively higher value of k of samples after LBTH pretreatment was related to their higher reaction efficiency and accessibility in comparison with HDP, which was caused by the de-crystallization and de-construction effects of LBTH pretreatment (Figure 2).

Figure 4a shows the aldehyde content of DANC under the same oxidation conditions (1.2 mol per mol of AGU). As expected, the transformation of the cellulose crystalline structure and the decrease of crystallinity were beneficial to the oxidation of cellulose. Furthermore, the properties of the prepared DANC are shown in Table 1. For all samples, the aldehyde content gradually increased with the increase of oxidation time from 12 to 48 h. Compared with materials without LBTH pretreatment, the content of aldehyde groups in pretreated materials clearly increased in the same oxidant concentration and reaction time. Among them (under the same oxidation conditions), the aldehyde group content of DANC with LBTH non-dissolving pretreatment for 30 and 60 min increased by around 15 and 30%, respectively. Compared with the samples without LBTH pretreatment (L0, 1.2 mol, 48 h), the oxidation time of the samples with LBTH non-dissolving pretreatment (L60, 1.2 mol, 24 h) was reduced by 50% with the same aldehyde group content. As expected, HDP after LBTH pretreatment achieved the efficient de-crystallization and de-construction effects, and the highly improved accessibility of HDP was conducive to promote the following $NaIO_4$ oxidation. As shown in Figure S4, the DANC prepared by LBTH pretreatment was evenly dispersed in water under the same oxidant concentration and reaction time. In contrast, the DANC without LBTH pretreatment was unevenly dispersed and opaque in water. For all samples, the zeta potential (absolute value) gradually increased with the increase of oxidation time from 12 to 48 h. The low value of the zeta potential may be caused by the effect of high-pressure homogenization, which exposed much more hydroxyl groups on the DANC surface. The dispersion of the obtained DANC with the increased zeta potential (absolute value) becomes more stable with the increase of oxidation time. The higher the content of aldehyde groups, the higher the charge density of the obtained DANC, leading to a homogeneous and stable dispersion of DANC in water. As shown in Figure 4c, the $NaIO_4$ oxidation in the molecular structure of the HDP was quantitatively determined by the liquid-state quantitative 13C NMR, and 4-nitrobenzaldehyde (10 mg/mL) was used as

Table 1. Effects of $NaIO_4$ Oxidation on Yield, Aldehyde Content, and Zeta Potential of DANC

LBTH pretreatment time (min)	$NaIO_4$ (mol per mol of AGU)	reaction time (h)	aldehyde content (mmol/g)	zeta potential (mV)	yield (%)
0	0.6	24	1.56	−21.12	96.5
	0.6	48	2.06	−23.25	95.3
	1.2	24	2.24	−23.26	96.5
	1.2	48	3.50	−28.40	95.1
30	0.6	12	1.35	−23.56	96.3
	0.6	24	1.73	−25.69	95.6
	0.6	36	2.32	−30.67	93.9
	0.6	48	2.53	−38.25	94.4
	1.2	12	2.67	−25.89	95.8
	1.2	24	3.26	−29.65	94.3
	1.2	36	3.69	−38.56	94.9
	1.2	48	4.03	−48.36	93.2
60	0.6	12	1.45	−25.36	95.1
	0.6	24	1.75	−26.89	94.5
	0.6	36	2.13	−35.56	94.1
	0.6	48	2.57	−40.25	93.4
	1.2	12	3.03	−27.86	94.1
	1.2	24	3.70	−33.00	93.6
	1.2	36	4.30	−46.93	93.1
	1.2	48	4.57	−53.06	92.8

https://doi.org/10.1021/acssuschemeng.2c07746
ACS Sustainable Chem. Eng. 2023, 11, 6641−6651

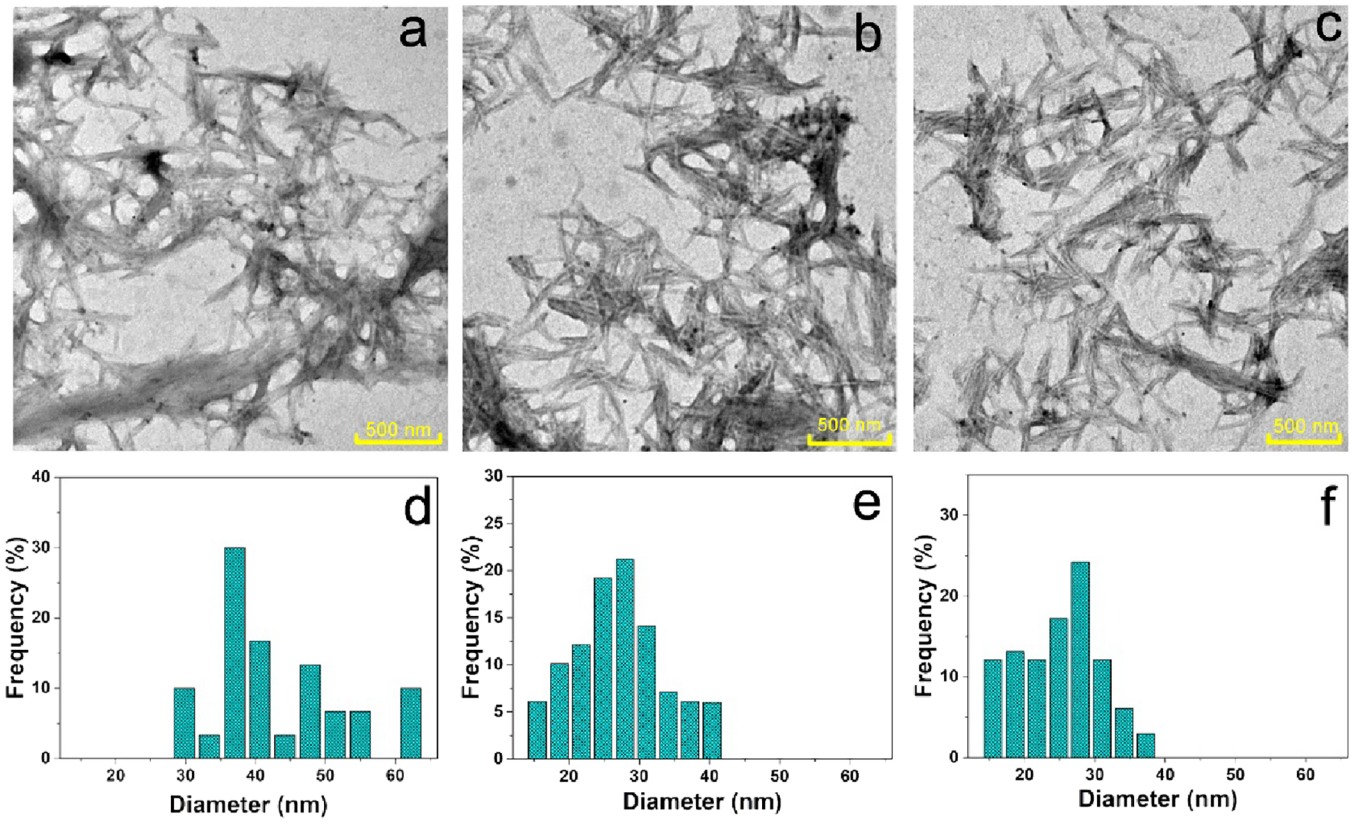

Figure 5. TEM images and diameter distribution of DANC. (a, d) L0, 1.2 mol, 48 h; (b, e) L30, 1.2 mol, 48 h; (c, f) L60, 1.2 mol, 48 h.

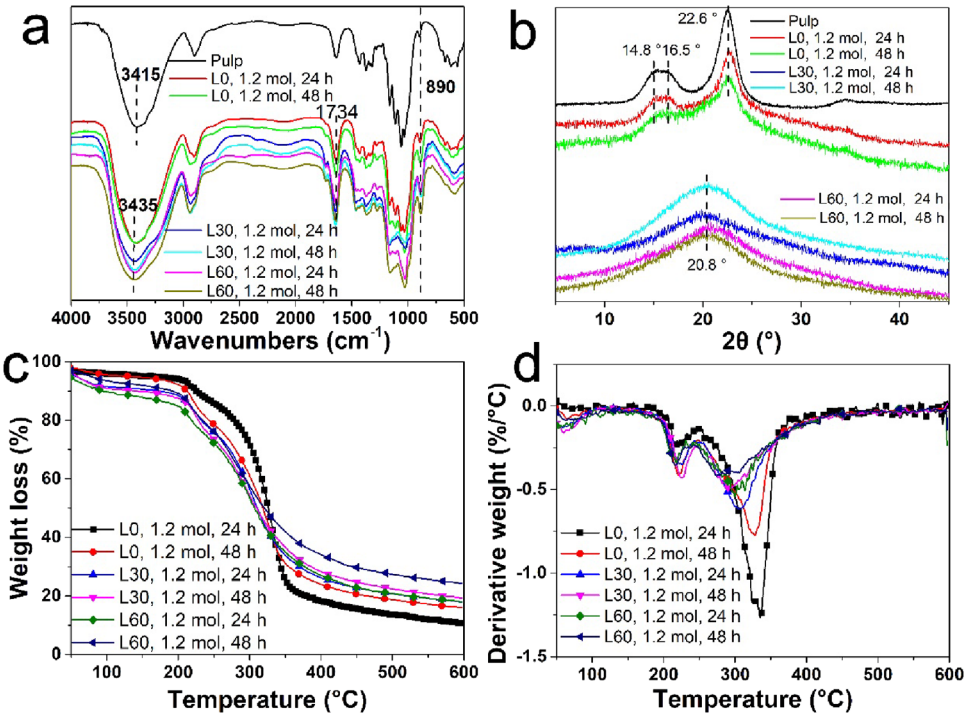

Figure 6. FTIR spectra (a), XRD patterns (b), and TG (c) and DTG (d) curves of pulp, oxidized pulp, and the oxidized sample after LBTH pretreatment.

internal standard. The signals in the NMR spectra of 100 to 106 ppm belong to anomeric carbon (C1), and the signals of 60 to 84 ppm belong to C2 to C6, which can be attributed to the HDP.[48] After $NaIO_4$ oxidation, the vicinal 2,3-hydroxyl groups of cellulose units can be oxidized to aldehyde groups (C2′ and C3′ at 165 to 167 ppm) and the hemiacetal formation of the aldehyde group (C2″ and C3″) can be detected at 92 and 99 ppm as well.[48] The 13C NMR presented

https://doi.org/10.1021/acssuschemeng.2c07746
ACS Sustainable Chem. Eng. 2023, 11, 6641−6651

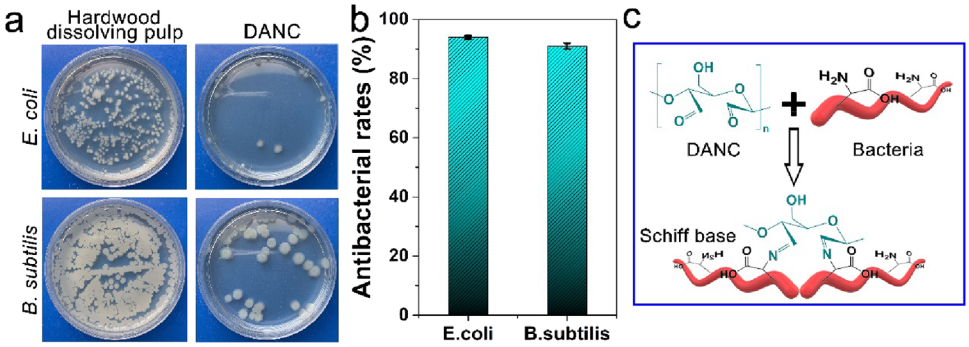

Figure 7. Antibacterial tests (a), antibacterial rates (b), and schematic diagram (c) of DANC.

a forest of peaks clustered mainly around the CH2−5 region, which was caused by the depolymerization of HDP. This phenomenon indicated that DANC was fragmented into glucose, cellobiose, and likely other oligomers during the preparation of the samples for liquid-state NMR (overnight under stirring), while polymeric cellulose also remained, which was caused by the significant instability of DANC.[49] The aldehyde content in oxidated samples was computed by the comparison of the sum of signal integration of C2′, C3′, C2″, and C3″ to internal standard (Figure 4c). The aldehyde contents of sample L0−1.2-48 and sample L60−1.2-48 were 0.74 and 0.89 mmol/g, respectively, which were in line with the data calculated by the titration approach.

Characterization of DANC. TEM images of the prepared DANC are shown in Figure 5. DANC with a diameter of 30−60 nm was prepared without LBTH pretreatment and presented a large microfibril bundle structure, which was attributed to the incomplete fibrillation (Figure 5a). However, it should be noted that the diameter of DANC decreased with the increase of LBTH pretreatment time. As shown in Figure 5e,f, DANC with a diameter of 15−40 nm was prepared after LBTH pretreatment, which was attributed to the fact that LBTH pretreatment was conducive to the subsequent $NaIO_4$ oxidation modification.

ATR-FTIR, XRD, and TG were also used to further investigate the molecular structural changes and thermal stability of cellulose after oxidation. As shown in Figure 6a, the band of O−H stretching vibration shifted to a higher wavenumber (from 3415 to 3435 cm^{-1}), which was caused by the reduced hydrogen bonding in cellulose after LBTH pretreatment.[39] Compared with the spectrum of HDP, there was a new absorption peak at 1734 cm^{-1} in the spectra of all $NaIO_4$-oxidized samples, which was due to the presence of C=O bonds in DANC samples.[50] In addition, the absorption peak at 890 cm^{-1} of all $NaIO_4$ oxidized samples was increased compared with that of HDP, which was caused by the formation of hemiacetal bonds between the aldehyde groups and adjacent hydroxyl groups.[48,49] As shown in Figure 6b, the crystalline structure of oxidized samples without LBTH pretreatment (such as HDP, the sample after $NaIO_4$ oxidized for 24 h, and the sample after $NaIO_4$ oxidized for 48 h) were cellulose Iβ (14.8, 16.5, and 22.6°).[36,37] However, after the LBTH pretreatment and oxidation process, the crystalline structure of LBTH-pretreated samples largely changed from cellulose Iβ (14.8, 16.5, and 22.6°) to amorphous structure (20.8°), and the crystallinity of cellulose clearly decreased due to the deconstruction and de-crystallinity effects of LBTH non-dissolving pretreatment.[34] Furthermore, as shown in Figure 6c,d, the T_o and T_{max} of HDP after $NaIO_4$ oxidation for 48 h were 264.1 and 329.1 °C, respectively. As evident, the T_o and T_{max} of the oxidized sample with LBTH non-dissolving pretreatment were lower than those of oxidized HDP without pretreatment. The T_o and T_{max} of oxidized samples with LBTH non-dissolving pretreatment for 60 min were only 231.6 and 284.3 °C, which was probably due to the relatively low crystallinity (36.6%) of samples and the strong oxidation effect of $NaIO_4$. Moreover, the increased residue amount of oxidized samples after LBTH pretreatment was caused by the strong oxidation effect of $NaIO_4$, leading to the easy formation of thermally stable char (Table S4).[43]

Antibacterial Tests. The antibacterial property of DANC was studied in comparison to HDP, and *Escherichia coli* (*E. coli*) and *Bacillus subtilis* (*B. subtilis*) were selected to represent the typical Gram-negative and Gram-positive bacteria. The antibacterial rates of DANC were 94 and 91% against *E. coli* and *B. subtilis* at concentrations of bacterium at 10^{-6} (Figure 7a,b), respectively, ascribed to the introduced aldehyde content that can efficiently inhibit the growth and multiplication of Gram-negative bacteria (*E. coli*) and Gram-positive bacteria (*B. subtilis*) via Schiff base reaction (Figure 7c).[51] Previous literatures reported that DANC combined with proteins and nucleic acids of bacteria by crosslinking results in the inactivation of microbes.[51] Therefore, DANC with excellent antibacterial properties had a great potential to be the functional material in antibacterial daily agents and medical supplies.

Salt Hydrate Reuse and Cost Analysis. The reuse and recycling of LBTH are very important in sustainable chemistry. Since cellulose was not dissolved in the LBTH pretreatment, the mixture was able to be easily separated into salt hydrate solution and cellulose and the obtained liquid after filtration can be directly reused in a new round of cellulose pretreatment steps without adding fresh salt. Subsequently, the LBTH with different recycling times was reused in the pretreatment of fresh HDP and the properties of DANC were investigated accordingly. As shown in Table 2, the aldehyde group content and zeta potential values of DANC were quite similar for all the reuse experiments. The results showed that LBTH maintained its effectiveness on the non-dissolving pretreatment of cellulose after the reuse and recycling process.

Furthermore, we did the cost analysis of periodate oxidation with and without LBTH pretreatment. As mentioned above, the obtained liquid after filtration can be directly reused in a new round of cellulose pretreatment steps without adding fresh salt. Also, the recovery and reuse of LBTH can further lower the cost of the LBTH non-dissolving pretreatment, and the

https://doi.org/10.1021/acssuschemeng.2c07746
ACS Sustainable Chem. Eng. 2023, 11, 6641−6651

Table 2. Evaluation of the Reuse of LBTH (L60, 1.2 mol, 48 h)

samples	LBTH recovered (%)	yield (%)	aldehyde content (mmol/g)	zeta potential (mV)
fresh LBTH		92.8	4.57 ± 0.05	−53.06 ± 0.18
first reuse	98	93.5	4.43 ± 0.16	−48.58 ± 0.21
second reuse	96	93.0	4.41 ± 0.11	−46.65 ± 0.11
third reuse	97	92.5	4.39 ± 0.08	−48.36 ± 0.26
fourth reuse	95	93.1	4.34 ± 0.15	−44.38 ± 0.15
fifth reuse	95	92.2	4.27 ± 0.07	−46.57 ± 0.29

cost of LBTH can be reduced to 1 $/kg based on the recycling of LBTH.[34] As shown in Table 3, to obtain the DANC with 1.4 mmol/g aldehyde content, the cost of periodate oxidation without LBTH non-dissolving pretreatment was around 50.24 $/kg-DANC. Nevertheless, the cost of DANC prepared with LBTH non-dissolving pretreatment for 60 min was lowered to 27.52 $/kg-DANC. That is around 45% reduction of operational cost compared with the traditional periodate oxidation method. It is worth pointing out that LBTH non-dissolving pretreatment can lead to 50% reduction of $NaIO_4$ dosage and 38% decreasing of the post homogenization time. Therefore, LBTH non-dissolving pretreatment can significantly reduce the operational cost of periodate oxidation for the preparation of DANC.

Mechanism of LBTH Non-Dissolving Pretreatment and Comparison of LBTH Pretreatment with Other Pretreatment Methods. Based on the analyses discussed above, the mechanism of the de-crystallization and de-construction effects of LBTH non-dissolving pretreatment on DHP and the following $NaIO_4$ oxidation was proposed (Figure 8). Lithium cations can act on the oxygen of cellulose hydroxyls and the hydroxyl groups of cellulose, breaking the hydrogen bonds of cellulose chains, while the bromine anion can bond with H of hydroxyl groups on cellulose to prevent the reconstruction of hydrogen bonds in the inter- and intra-molecular bonds of cellulose. After LBTH pretreatment, the crystalline structure of HDP was changed from cellulose Iβ to amorphous structure (Figure 2) and the hydrogen bonding of cellulose was weakened after LBTH pretreatment (Figure 3 and Figure S3). Under the above effect, the tight cellulose structure was significantly altered after LBTH non-dissolving pretreatment (Figure 2). After that, the vicinal 2,3-hydroxyl groups of cellulose units can be oxidized to aldehyde groups with the highly improved accessibility of the LBTH-pretreated DHP. These relatively low crystallinity and opened structures of cellulose significantly increased the accessibility, thus leading to an upgraded approach with less energy and chemical consumption and lower cost (45% reduction) for the preparation of DANC through LBTH non-dissolving pretreatment.

Finally, comparison of LBTH pretreatment with other pretreatment methods was investigated, in terms of cost, temperature, time, concentration, and recyclability (Figure 8b). The above pretreatment methods, including enzymes, dilute acid, alkali, ILs, and DESs, do have several drawbacks like long pretreatment time, environmental issues, high pretreated temperature, low pretreated concentration, and high cost of enzymes or chemicals, which was unsustainable for large-scale application. For instance, the pretreatment time of enzymes was almost 72 h, which was nearly 144 times longer than that of LBTH pretreatment. Also, the pretreatment temperature of dilute acid (180 °C) was nearly seven times higher than that of LBTH pretreatment (25 °C). Moreover, the cost of LBTH can be reduced to 1 $/kg based on the recycling of LBTH,[34] which was lower than that of other pretreatment methods. Therefore, it can be concluded that LBTH pretreatment with the advantages of easy recycling and reuse, low cost, high efficiency, and sustainability can be a promising and competitive strategy for the improvement of cellulose accessibility, guaranteeing a safer and more cost-effective process for cellulose modification.

CONCLUSIONS

Development of sustainable and effective pretreatment methods is very important for hydrolysis or functional modification of cellulose, which is of vital importance for its final utilization. In this work, a novel approach with less energy and chemical consumption was developed for the preparation of DANC through LBTH pretreatment to improve the accessibility of cellulose. Results indicated that LBTH significantly improved the accessibility of cellulose and the efficiency of $NaIO_4$ oxidation. The *CrI* of the LBTH-pretreated HDP was reduced from 83.2 to 48.7%, and the hydrogen bonding of cellulose was clearly weakened after LBTH non-dissolving pretreatment. The aldehyde group content of the obtained DANC increased by around 15 and 30% for the ones with LBTH non-dissolving pretreatment for 30 and 60 min, respectively. Compared with the samples without LBTH non-dissolving pretreatment (L0, 1.2 mol, 48 h), the oxidation time of the samples with LBTH pretreatment (L60, 1.2 mol, 24 h) was reduced by 50% with the same aldehyde group content. Additionally, LBTH can be easily recovered and reused and the recycling did not affect the effectiveness of the LBTH pretreatment. Also, the prepared DANC displayed excellent antibacterial properties against both *E. coli* and *B. subtilis* because of the presence of sufficient aldehyde groups. Thus, this simple, sustainable, and cost-effective LBTH non-dissolving pretreatment is a good approach for improvement

Table 3. Comparison of Operational Cost ($/kg-DANC) of DANC Prepared from HDP with or without LBTH Pretreatment

methods	LBTH pretreated ($/kg)	chemical cost[a] ($/kg)	energy cost[b] ($/kg)	homogenization cost[c] ($/kg)	aldehyde content (mmol/g)	production cost ($/kg)
periodate oxidation	0	45.71	0.81	2.24	1.48	50.24
periodate oxidation (LBTH 60 min)	1	22.86	0.81	1.40	1.45	27.52

[a]The $NaIO_4$ cost was estimated at 45.71 $/kg DANC (1.2 mol per mol of AGU). [b]The energy cost was calculated as 0.1 $/kWh.[52] [c]The homogenization cost of traditional periodate oxidation was estimated at 2.24 $/kg DANC (eight times at 600 bars); the homogenization cost of periodate oxidation with LBTH pretreatment was estimated at 1.4 $/kg DANC (5 times at 600 bars).

https://doi.org/10.1021/acssuschemeng.2c07746
ACS Sustainable Chem. Eng. 2023, 11, 6641−6651

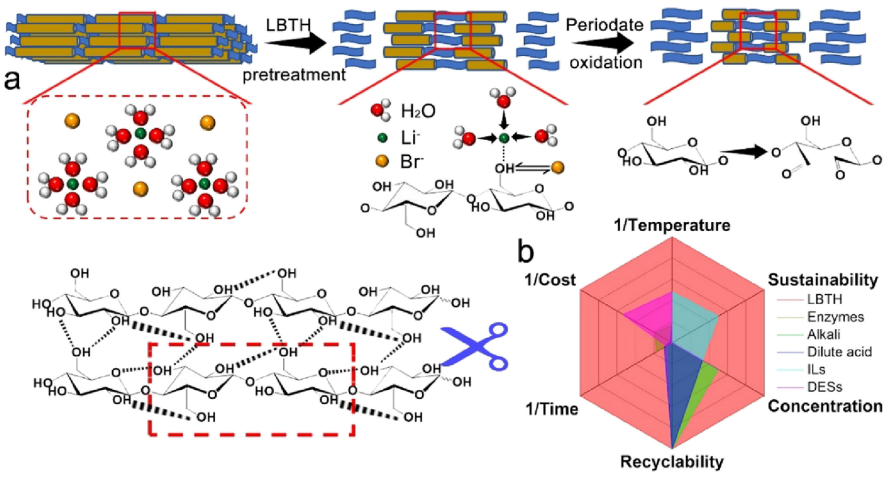

Figure 8. (a) Mechanism for the effect of LBTH non-dissolving pretreatment and the promotion of periodate oxidation. (b) Comparison of LBTH pretreatment with other pretreatment methods (detailed data is listed in Table S5).

of cellulose accessibility, promoting cleaner modifications of cellulose and boosting the utilizations of cellulose materials.

■ ASSOCIATED CONTENT

Supporting Information

The Supporting Information is available free of charge at https://pubs.acs.org/doi/10.1021/acssuschemeng.2c07746.

Detailed characterization methods and kinetic study of DANC, yield of cellulose after LBTH non-dissolving pretreatment (Figure S1), SEM images of cellulose samples (Figure S2), peak-differentiating and imitating of FTIR spectra (Figure S3), picture of the prepared DANC samples (Figure S4), thermogravimetric data of HDP and the samples after LBTH non-dissolving pretreatment (Table S1), values of x and Y at different reaction orders for different samples (Table S2), values of n, k, and R^2 of oxidated HDP and the oxidated sample with LBTH non-dissolving pretreatment (Table S3), thermogravimetric data of HDP and the oxidated sample after LBTH non-dissolving pretreatment (Table S4), comparison of LBTH pretreatment with other pretreatment methods in terms of cost, temperature, time, concentration, and recyclability, including enzymes, dilute acid, alkali, ILs, and DESs treatment (Table S5) (PDF)

■ AUTHOR INFORMATION

Corresponding Authors

Chunlin Xu − *Laboratory of Natural Materials Technology, Åbo Akademi University, Turku FI-20500, Finland*; Email: Chunlin.Xu@abo.fi

Bin Li − *CAS Key Laboratory of Biofuels, Qingdao Institute of Bioenergy and Bioprocess Technology, Chinese Academy of Sciences, Qingdao 266101, PR China; Shandong Energy Institute, Qingdao 266101, PR China; Qingdao New Energy Shandong Laboratory, Qingdao 266101, PR China;* orcid.org/0000-0002-8903-3874; Email: libin@qibebt.ac.cn

Authors

Yidong Zhang − *CAS Key Laboratory of Biofuels, Qingdao Institute of Bioenergy and Bioprocess Technology, Chinese Academy of Sciences, Qingdao 266101, PR China; Laboratory of Natural Materials Technology, Åbo Akademi University, Turku FI-20500, Finland;* orcid.org/0000-0003-4070-8276

Wangfang Deng − *CAS Key Laboratory of Biofuels, Qingdao Institute of Bioenergy and Bioprocess Technology, Chinese Academy of Sciences, Qingdao 266101, PR China; Laboratory of Natural Materials Technology, Åbo Akademi University, Turku FI-20500, Finland*

Chao Liu − *CAS Key Laboratory of Biofuels, Qingdao Institute of Bioenergy and Bioprocess Technology, Chinese Academy of Sciences, Qingdao 266101, PR China*

Fei Yan − *CAS Key Laboratory of Biofuels, Qingdao Institute of Bioenergy and Bioprocess Technology, Chinese Academy of Sciences, Qingdao 266101, PR China*

Meiyan Wu − *CAS Key Laboratory of Biofuels, Qingdao Institute of Bioenergy and Bioprocess Technology, Chinese Academy of Sciences, Qingdao 266101, PR China; Shandong Energy Institute, Qingdao 266101, PR China*

Qiu Cui − *CAS Key Laboratory of Biofuels, Qingdao Institute of Bioenergy and Bioprocess Technology, Chinese Academy of Sciences, Qingdao 266101, PR China; Shandong Energy Institute, Qingdao 266101, PR China; Qingdao New Energy Shandong Laboratory, Qingdao 266101, PR China*

Stefan Willför − *Laboratory of Natural Materials Technology, Åbo Akademi University, Turku FI-20500, Finland*

Complete contact information is available at: https://pubs.acs.org/10.1021/acssuschemeng.2c07746

Author Contributions

#Y.Z. and W.D. contributed equally.

Author Contributions

Y.Z. and W.D. carried out most experiments, conceived the concept, and co-wrote the manuscript. B.L., C.X., S.W., and Q.C. supervised the work. B.L., C.X., and S.W. revised the manuscript. C.L., F.Y., and M.W. contributed to the sample preparation and discussed the results. All authors commented on the submitted version of the manuscript.

Notes

The authors declare no competing financial interest.

https://doi.org/10.1021/acssuschemeng.2c07746
ACS Sustainable Chem. Eng. 2023, 11, 6641−6651

■ ACKNOWLEDGMENTS

This work was financially supported by the National Natural Science Foundation of China (No. U22A20423 and No. 22208358), the Strategic Priority Research Program of the Chinese Academy of Sciences (No. XDA21061012), the Qingdao Independent Innovation Major Project (No. 21-1-2-23-hz), and the Shandong Energy Institute Research Foundation (No. SEI S202106). In addition, Y.Z. acknowledges the financial support from the China Scholarship Council (No. 202207960008).

■ ABBREVIATIONS

$NaIO_4$, sodium periodate; DANC, dialdehyde nanocellulose; LBTH, lithium bromide trihydrate; HDP, hardwood dissolving pulp; ILs, ionic liquids; DESs, deep eutectic solvent pretreatment; MSH, molten salt hydrates; MCC, microcrystalline cellulose; LiBr, lithium bromide; LB, Luria-Bertani

■ REFERENCES

(1) Guo, Z.; Zhang, Q.; You, T.; Zhang, X.; Xu, F.; Wu, Y. Short-Time Deep Eutectic Solvent Pretreatment for Enhanced Enzymatic Saccharification and Lignin Valorization. *Green Chem.* **2019**, *21*, 3099−3108.
(2) Zhao, D.; Zhu, Y.; Cheng, W.; Chen, W.; Wu, Y.; Yu, H. Cellulose-Based Flexible Functional Materials for Emerging Intelligent Electronics. *Adv. Mater.* **2021**, *33*, 2000619.
(3) Xu, R.; Du, H. S.; Liu, C.; Liu, H. Y.; Wu, M. Y.; Zhang, X. Y.; Si, C. L.; Li, B. An Efficient and Magnetic Adsorbent Prepared in A Dry Process with Enzymatic Hydrolysis Residues for Wastewater Treatment. *J. Cleaner Prod.* **2021**, *313*, No. 127834.
(4) Sun, Y.; Chu, Y.; Wu, W.; Xiao, H. Nanocellulose-Based Lightweight Porous Materials: A Review. *Carbohydr. Polym.* **2021**, *255*, 117489−117489.
(5) Wu, M.; Yu, G.; Chen, W.; Dong, S.; Wang, Y.; Liu, C.; Li, B. A Pulp Foam with Highly Improved Physical Strength, Fire-Resistance and Antibiosis by Incorporation of Chitosan and CPAM. *Carbohydr. Polym.* **2022**, *278*, 118936.
(6) Zhang, Y.; Deng, W.; Wu, M.; Liu, Z.; Yu, G.; Cui, Q.; Liu, C.; Fatehi, P.; Li, B. Robust, Scalable, and Cost-Effective Surface Carbonized Pulp Foam for Highly Efficient Solar Steam Generation. *ACS Appl. Mater. Interfaces* **2023**, *15*, 7414−7426.
(7) El Meligy, M. G.; El Rafie, S.; Abu-Zied, K. M. Preparation of Dialdehyde Cellulose Hydrazone Derivatives and Evaluating Their Efficiency for Sewage Wastewater Treatment. *Desalination* **2005**, *173*, 33−44.
(8) Jin, L.; Sun, Q.; Xu, Q.; Xu, Y. Adsorptive Removal of Anionic Dyes from Aqueous Solutions using Microgel Based on Nanocellulose and Polyvinylamine. *Bioresour. Technol.* **2015**, *197*, 348−355.
(9) Yu, D.; Wang, Y.; Wu, M.; Zhang, L.; Wang, L.; Ni, H. Surface Functionalization of Cellulose with Hyperbranched Polyamide for Efficient Adsorption of Organic Dyes and Heavy Metals. *J. Cleaner Prod.* **2019**, *232*, 774−783.
(10) Pietrucha, K.; Safandowska, M. Dialdehyde Cellulose-Cross-linked Collagen and Its Physicochemical Properties. *Process Biochem.* **2015**, *50*, 2105−2111.
(11) Keshk, S. M. A. S.; Ramadan, A. M.; Bondock, S. Physicochemical Characterization of Novel Schiff Bases Derived from Developed Bacterial Cellulose 2,3-dialdehyde. *Carbohydr. Polym.* **2015**, *127*, 246−251.
(12) Zhang, X.; Shen, G.; Sun, S.; Shen, Y.; Zhang, C.; Xiao, A. Direct Immobilization of Antibodies on Dialdehyde Cellulose Film for Convenient Construction of an Electrochemical Immunosensor. *Sens. Actuators, B* **2014**, *200*, 304−309.
(13) Verma, V.; Verma, P.; Ray, P.; Ray, A. R. 2, 3-Dihydrazone Cellulose: Prospective Material for Tissue Engineering Scaffolds. *Mater. Sci. Eng., C: Biomimetic Supramol. Syst.* **2008**, *28*, 1441−1447.
(14) Luo, H.; Lan, H.; Cha, R.; Yu, X.; Gao, P.; Zhang, P.; Zhang, C.; Han, L.; Jiang, X. Dialdehyde Nanocrystalline Cellulose as Antibiotic Substitutes against Multidrug-Resistant Bacteria. *ACS Appl. Mater. Interfaces* **2021**, *13*, 33802−33811.
(15) Tian, X.; Jiang, X. Preparing Water-Soluble 2, 3-Dialdehyde Cellulose as A Bio-Origin Cross-Linker of Chitosan. *Cellulose* **2018**, *25*, 987−998.
(16) Wang, B.; Ma, C.; Fu, L. H.; Ji, X. X.; Jing, F. C.; Liu, S.; Ma, M. G. Synthesis and Characterization of Dialdehyde Cellulose/Silver Composites by Microwave-assisted Hydrothermal Method. *BioResources* **2018**, *13*, 5793−5804.
(17) Hu, Y.; Li, N.; Yue, P.; Chen, G.; Hao, X.; Bian, J.; Peng, F. Highly Antibacterial Hydrogels Prepared from Amino Cellulose, Dialdehyde Xylan, and Ag Nanoparticles by A Green Reduction Method. *Cellulose* **2022**, *29*, 1055−1067.
(18) Al-Abri, S. S.; Said, S. A.; Al Touby, S. S.; Hossain, M. A.; Al-Sabahi, J. N. Composition Analysis and Antimicrobial Activity of Essential Oil from Leaves of Laurus Nobilis Grown in Oman. *J. Bioresource Bioprod.* **2022**, *7*, 328−334.
(19) Deng, C.; Seidi, F.; Yong, Q.; Jin, X.; Li, C.; Zhang, X.; Han, J. Q.; Liu, Y.; Huang, Y.; Wang, Y.; Yuan, Z.; Xiao, H. Antiviral/antibacterial Biodegradable Cellulose Nonwovens as Environmentally Friendly and Bioprotective Materials with Potential to Minimize Microplastic Pollution. *J. Hazard. Mater.* **2022**, *424*, No. 127391.
(20) Pang, B.; Liu, H.; Rehfeldt, F.; Zhang, K. High Internal Phase Pickering Emulsions Stabilized by Dialdehyde Amylopectin/Chitosan Complex Nanoparticles. *Carbohydr. Polym.* **2021**, *258*, No. 117655.
(21) Dang, X.; Liu, P.; Yang, M.; Deng, H.; Shan, Z.; Zhen, W. Production and Characterization of Dialdehyde Cellulose through Green and Sustainable Approach. *Cellulose* **2019**, *26*, 9503−9515.
(22) Munster, L.; Vicha, J.; Klofac, J.; Masar, M.; Kucharczyk, P.; Kuritka, I. Stability and aging of solubilized dialdehyde cellulose. *Cellulose* **2017**, *24*, 2753−2766.
(23) Liimatainen, H.; Sirvio, J.; Pajari, H.; Hormi, O.; Niinimaki, J. Regeneration and Recycling of Aqueous Periodate Solution in Dialdehyde Cellulose Production. *J. Wood Chem. Technol.* **2013**, *33*, 258−266.
(24) Miao, J.; Yu, Y.; Jiang, Z.; Zhang, L. One-pot Preparation of Hydrophobic Cellulose Nanocrystals in An Ionic Liquid. *Cellulose* **2016**, *23*, 1209−1219.
(25) Sirvio, J. A.; Visanko, M.; Liimatainen, H. Acidic Deep Eutectic Solvents As Hydrolytic Media for Cellulose Nanocrystal Production. *Biomacromolecules* **2016**, *17*, 3025−3032.
(26) Li, N.; Bian, H. Y.; Zhu, J. Y.; Ciesielski, P. N.; Pan, X. J. Tailorable Cellulose II Nanocrystals (CNC II) Prepared in Mildly Acidic Lithium Bromide Trihydrate (MALBTH)Dagger. *Green Chem.* **2021**, *23*, 2778−2791.
(27) Rodriguez Quiroz, N.; Padmanathan, A. M. D.; Mushrif, S. H.; Vlachos, D. G. Understanding Acidity of Molten Salt Hydrate Media for Cellulose Hydrolysis by Combining Kinetic Studies, Electrolyte Solution Modeling, Molecular Dynamics Simulations, and C-13 NMR Experiments. *ACS Catal.* **2019**, *9*, 10551−10561.
(28) Liao, Y.; Pang, Z. Q.; Pan, X. Fabrication and Mechanistic Study of Aerogels Directly from Whole Biomass. *ACS Sustainable Chem. Eng.* **2019**, *7*, 17723−17736.
(29) Quiroz, N. R.; Norton, A. M.; Nguyen, H.; Vasileiadou, E.; Vlachos, D. G. Homogeneous Metal Salt Solutions for Biomass Upgrading and Other Select Organic Reactions. *ACS Catal.* **2019**, *9*, 9923−9952.
(30) Sen, S.; Martin, J. D.; Argyropoulos, D. S. Review of Cellulose Non-Derivatizing Solvent Interactions with Emphasis on Activity in Inorganic Molten Salt Hydrates. *ACS Sustainable Chem. Eng.* **2013**, *1*, 858−870.
(31) Burger, D.; Winter, A.; Subbiandoss, G.; Oberlerchner, J. T.; Beaumont, M.; Tamada, Y.; Rosenau, T. Partial Amorphization of Cellulose through Zinc Chloride Treatment: A Facile and Sustainable Pathway to Functional Cellulose Nanofibers with Flame-Retardant and Catalytic Properties. *ACS Sustainable Chem. Eng.* **2020**, *8*, 13576−13582.

https://doi.org/10.1021/acssuschemeng.2c07746
ACS Sustainable Chem. Eng. 2023, 11, 6641−6651

(32) Yang, Y. J.; Shin, J. M.; Kang, T. H.; Kimura, S.; Wada, M.; Kim, U. J. Cellulose Dissolution in Aqueous Lithium Bromide Solutions. *Cellulose* **2014**, *21*, 1175−1181.
(33) Li, N.; Pan, X.; Alexander, J. A Facile and Fast Method for Quantitating Lignin in Lignocellulosic Biomass using Acidic Lithium Bromide Trihydrate (ALBTH). *Green Chem.* **2016**, *18*, 5367−5376.
(34) Huang, Z.; Yu, G.; Liu, C.; Wu, M.; Tang, Y.; Li, B.; Peng, H. Ultrafast Improvement of Cellulose Accessibility via Non-Dissolving Pretreatment with $LiBr{\cdot}3H_2O$ under Room Temperature. *Carbohydr. Polym.* **2022**, *284*, No. 119180.
(35) Kang, X.; Deng, L.; Yi, L.; Ruan, C.-Q.; Zeng, K. A Facile Method for Preparation of Green and Antibacterial Hydrogel Based on Chitosan and Water-Soluble 2,3-Dialdehyde Cellulose. *Cellulose* **2021**, *28*, 6403−6416.
(36) Zhang, Y.; Liu, C.; Wu, M.; Li, Z.; Li, B. Impact of the Incorporation of Nano-Sized Cellulose Formate on the End Quality of Polylactic Acid Composite Film. *Nanomaterials* **2022**, *12*, 1.
(37) Zhang, Y.; Wang, J.; Liu, C.; Liu, Y.; Li, Y.; Wu, M.; Li, Z.; Li, B. Influence of Drying Methods on The Structure and Properties of Cellulose Formate and Its Application as A Reducing Agent. *Int. J. Biol. Macromol.* **2021**, *170*, 397−405.
(38) Lu, R.; Zhang, X.; Fu, L.; Wang, H.; Briber, R. M.; Wang, H. Amorphous Cellulose Thin Films. *Cellulose* **2020**, *27*, 2959−2965.
(39) Chen, C. Y.; Chen, M. J.; Zhang, X. Q.; Liu, C. F.; Sun, R. C. Per-O-acetylation of Cellulose in Dimethyl Sulfoxide with Catalyzed Transesterification. *J. Agric. Food Chem.* **2014**, *62*, 3446−3452.
(40) Hishikawa, Y.; Togawa, E.; Kondo, T. Characterization of Individual Hydrogen Bonds in Crystalline Regenerated Cellulose Using Resolved Polarized FTIR Spectra. *ACS Omega* **2017**, *2*, 1469−1476.
(41) Liang, C. Y.; Marchessault, R. H. Infrared Spectra of Crystalline Polysaccharides. I. Hydrogen Bonds in Native Celluloses. *J. Polym. Sci.* **1959**, *37*, 385−395.
(42) Li, B.; Xu, W.; Kronlund, D.; Maattanen, A.; Liu, J.; Smatt, J.; Peltonen, J.; Willfor, S.; Mu, X.; Xu, C. Cellulose Nanocrystals Prepared via Formic Acid Hydrolysis Followed by TEMPO-Mediated Oxidation. *Carbohydr. Polym.* **2015**, *133*, 605−612.
(43) Koklukaya, O.; Carosio, F.; Wagberg, L. Tailoring Flame-Retardancy and Strength of Papers via Layer-By-Layer Treatment of Cellulose Fibers. *Cellulose* **2018**, *25*, 2691−2709.
(44) Li, Z.; Hu, P.; Yu, J.; Hu, Z.; Liu, Z. Preparation and Characterization of Regenerated Cellulose Fibers from A Novel Solvent System. *J. Macromol. Sci., Part B: Phys.* **2008**, *47*, 288−295.
(45) Idstrom, A.; Brelid, H.; Nyden, M.; Nordstierna, L. CP/MAS C-13 NMR Study of Pulp Hornification Using Nanocrystalline Cellulose As a Model System. *Carbohydr. Polym.* **2013**, *92*, 881−884.
(46) Park, S.; Johnson, D. K.; Ishizawa, C. I.; Parilla, P. A.; Davis, M. F. Measuring The Crystallinity Index of Cellulose by Solid State C-13 Nuclear Magnetic Resonance. *Cellulose* **2009**, *16*, 641−647.
(47) Lv, D.; Du, H.; Che, X.; Wu, M.; Zhang, Y.; Liu, C.; Nie, S.; Zhang, X.; Li, B. Tailored and Integrated Production of Functional Cellulose Nanocrystals and Cellulose Nanofibrils via Sustainable Formic Acid Hydrolysis: Kinetic Study and Characterization. *ACS Sustainable Chem. Eng.* **2019**, *7*, 9449−9463.
(48) Wang, Q.; Xu, W.; Koppolu, R.; van Bochove, B.; Seppala, J.; Hupa, L.; Willfor, S.; Xu, C.; Wang, X. Injectable Thiol-Ene Hydrogel of Galactoglucomannan and Cellulose Nanocrystals in Delivery of Therapeutic Inorganic Ions with Embedded Bioactive Glass Nanoparticles. *Carbohydr. Polym.* **2022**, *276*, No. 118780.
(49) Koso, T.; del Cerro, D. R.; Heikkinen, S.; Nypelo, T.; Buffiere, J.; Perea-Buceta, J. E.; Potthast, A.; Rosenau, T.; Heikkinen, H.; Maaheimo, H.; Isogai, A.; Kilpelainen, I.; King, A. W. T. 2D Assignment and Quantitative Analysis of Cellulose and Oxidized Celluloses using Solution-State NMR Spectroscopy. *Cellulose* **2020**, *27*, 7929−7953.
(50) Abou-Yousef, H.; Dacrory, S.; Hasanin, M.; Saber, E.; Kamel, S. Biocompatible Hydrogel Based on Aldehyde-Functionalized Cellulose and Chitosan for Potential Control Drug Release. *Sustainable Chem. Pharm.* **2021**, *21*, No. 100419.
(51) Zhang, L. M.; Ge, H. H.; Xu, M.; Cao, J.; Dai, Y. J. Physicochemical Properties, Antioxidant and Antibacterial Activities of Dialdehyde Microcrystalline Cellulose. *Cellulose* **2017**, *24*, 2287−2298.
(52) Wang, C.; Zhou, K.; Yang, S. A Review of Residential Tiered Electricity Pricing in China. *Renew. Sust. Energy Rev.* **2017**, *79*, 533−543.

https://doi.org/10.1021/acssuschemeng.2c07746
ACS Sustainable Chem. Eng. 2023, 11, 6641−6651